J Neurophysiol 94: 567–575, 2005.
First published March 9, 2005; doi:10.1152/jn.00896.2004.

Regional and Laminar Differences in In Vivo Firing Patterns of Primate Cortical Neurons

Shigeru Shinomoto,[1] Youichi Miyazaki,[1,3] Hiroshi Tamura,[2] and Ichiro Fujita[2]

[1]*Graduate School of Science, Kyoto University, Kyoto;* [2]*Graduate School of Frontier Biosciences, Osaka University, Osaka; and* [3]*Hitachi, Totsuka, Yokohama, Japan*

Submitted 30 August 2004; accepted in final form 7 March 2005

Shinomoto, Shigeru, Youichi Miyazaki, Hiroshi Tamura, and Ichiro Fujita. Regional and laminar differences in in vivo firing patterns of primate cortical neurons. *J Neurophysiol* 94: 567–575, 2005. First published March 9, 2005; doi:10.1152/jn.00896.2004. The firing rates of cortical neurons change in time; yet, some aspects of their in vivo firing characteristics remain unchanged and are specific to individual neurons. A recent study has shown that neurons in the monkey medial motor areas can be grouped into 2 firing types, "likely random" and "quasi-regular," according to a measure of local variation of interspike intervals. In the present study, we extended this analysis to area TE of the inferior temporal cortex and addressed whether this classification applies generally to different cortical areas and whether different types of neurons show different laminar distribution. We found that area TE did consist of 2 groups of neurons with different firing characteristics, one similar to the "likely random" type in the medial motor cortical areas, and the other exhibiting a "clumpy-bursty" firing pattern unique to TE. The quasi-regular type was rarely observed in area TE. The likely random firing type of neuron was more frequently found in layers V–VI than in layers II–III, whereas the opposite was true for the clumpy-bursty firing type. These results show that neocortical areas consist of heterogeneous neurons that differ from one area to another in their basic firing characteristics. Moreover, we show that spike trains obtained from a single cortical neuron can provide a clue that helps to identify its layer localization.

INTRODUCTION

Neurophysiological studies have succeeded in correlating the firing activity of specific populations of neurons to animal behaviors, defining sites with neuronal activity in particular behavioral contexts as the functional areas corresponding to those behaviors. Although such observations are interesting in themselves, these studies do not necessarily examine neuronal activity in the context of circuitry. To address this question, information regarding not only neuronal activity but also cell type and location of individual neurons is required. Extracellularly recorded spike sequences can provide information that allows us to distinguish between cell types. In the hippocampus, for example, the firing rate of an interneuron is typically higher than that of a pyramidal neuron (Buzsáki et al. 1983; Ranck 1973) and, in the neocortex, there is a difference in the action potential waveform between pyramidal neurons and a specific class of interneurons (Constantinidis et al. 2002; Csicsvari et al. 1998; Mountcastle et al. 1969).

We have recently shown that the analysis of firing patterns can be used to classify neocortical neurons into distinct groups (Shinomoto et al. 2003). In that study, we compared the conventional coefficient of variation (*Cv*) and a newly introduced measure of time-local variation (*Lv*) of the recorded sequences of interspike intervals (ISIs). *Cv* reflects the global variability of an entire neuronal spike sequence and is sensitive to fluctuations in the firing rate. *Lv*, on the other hand, reflects the local stepwise variability of ISIs, depends less on the firing rate, and robustly represents the firing characteristics specific to individual neurons. Neurons in the medial motor areas (the presupplementary motor area, supplementary motor area, and rostral cingulate motor area) have been categorized into 2 distinct groups with different values of *Lv*. One group has an *Lv* of 0.81 on average and tends to fire in a random fashion and the other group has an *Lv* of 0.38 whose firing pattern is quasi-regular. The 2 groups of neurons classified according to their *Lv* values exhibit different responses to the same stimulus, with a significant difference in their onset latency. In contrast, no clear categorization is made on the basis of the *Cv* distribution.

Different cortical areas share many of the firing statistics, such as the dynamic range of responses and the spike count variance (Shadlen and Newsome 1998). It is unknown, however, whether the classification of neurons in the medial motor areas also applies to other cortices. In addition, it is unclear whether the 2 groups of neurons are intermingled or tend to cluster in separate locations in the gray matter, exhibiting separate localization in different layers, for instance. In the present study, we analyzed spike sequences recorded from area TE of the inferior temporal cortex of macaque monkeys. Histological markings made for each electrode penetration allowed for layer localization of the recorded position. Independently of this laminar location assignment, the recorded spike sequences were analyzed with respect to *Cv* and *Lv*. As in the medial motor areas, the distribution of *Lv* values was bimodal, whereas the distribution of *Cv* values was unimodal. The distribution peaks for TE neurons differed substantially from those of medial motor cortical neurons. The neurons exhibiting firing patterns with higher *Lv* values were mostly located in layers II–III, whereas those with lower *Lv* values were principally found in layers V–VI.

METHODS

Neurophysiological experiment

Here we briefly review the experiment described by Tamura et al. (2004). We applied our present analysis to these data.

Address for reprint requests and other correspondence: S. Shinomoto, Department of Physics, Graduate School of Science, Kyoto University, Sakyo-ku, Kyoto 606-8502, Japan (E-mail: shinomoto@scphys.kyoto-u.ac.jp).

The costs of publication of this article were defrayed in part by the payment of page charges. The article must therefore be hereby marked "*advertisement*" in accordance with 18 U.S.C. Section 1734 solely to indicate this fact.

Neuronal responses were recorded from area TE of the inferior temporal cortex in 4 anesthetized monkeys (*Macaca fuscata*; body weight, 5.2–7.5 kg). All the experimental procedures conformed to the guidelines of the National Institutes of Health (1996) and were approved by the animal experiment committee of Osaka University. General experimental procedures have been described elsewhere (Tamura et al. 2004). Monkeys were prepared for repeated recordings through an initial aseptic surgery under sodium pentobarbital surgical anesthesia.

Monkeys were anesthetized with nitrous oxide and isoflurane during recordings. Body temperature was maintained at 37–38°C. End-tidal CO_2 was kept at 4.0–4.5%. Electrocardiogram and arterial oxygen saturation levels were continuously monitored throughout the experiment. Eyes were dilated, covered with preselected contact lenses, and irrigated with saline.

Multiple single-unit recordings were made from area TE using a single-shaft electrode with 7 recording probes (Heptode; Thomas, Esslingen, Germany) (Fig. 1, *A* and *B*). Monkeys were paralyzed with pancuronium bromide during electrophysiological recordings. Recordings were made at intervals of $\geq$300 μm along a penetration axis. In every penetration, sampling was made throughout the gray matter from layer 2 to layer 6. All neurons encountered were recorded and analyzed. Isolation and classification of spikes from recorded signals were carried out off-line by an automated method (Kaneko et al. 1999).

Histology

For each penetration, 2 or 3 small electrolytic lesions were made by passing a cathodal current of 10 μA through the electrode tip for 10 s to allow later histological verification of the recording sites (Fig. 1*C*). After completion of the final recordings, monkeys were deeply anesthetized using sodium pentobarbital and perfused transcardially. The brain was cut into 100-μm-thick serial sections. All the electrolytic lesions were successfully recovered from Nissl-stained sections. We determined the laminar positions of the recording sites using a combination of the electrolytic lesions and the electrode manipulator readings noted for each recording site. Like other neocortical areas in monkeys, area TE exhibits a clear 6-layer organization (Fig. 1*C*). Identification of layers was based on the description of Fujita and Fujita (1996).

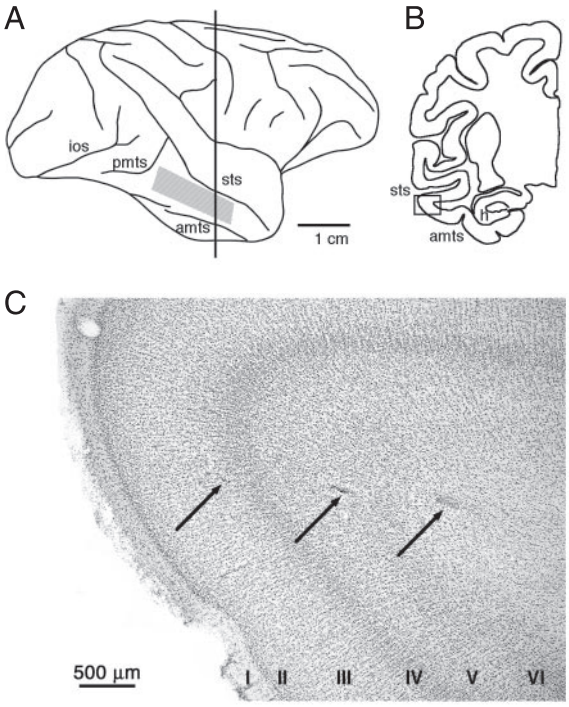

FIG. 1. *A* and *B*: recording sites are indicated as a shaded region in the lateral view of the right hemisphere (*A*) and as a box in a frontal section (*B*) taken at the level indicated by the vertical line in *A*. *C*: photograph of a Nissl-stained section of a portion of area TE indicated by the box in *B*. Arrows indicate the 3 electrolytic lesions made along a recording penetration. amts, anterior middle temporal sulcus; h, hippocampus; ios, inferior occipital sulcus; pmts, posterior middle temporal sulcus; sts, superior temporal sulcus.

Visual stimuli

The stimulus set consisted of 64 visual stimuli (53 geometrical shapes and 11 photographs of natural or man-made objects; see Fig. 1 of Tamura et al. 2004). Images were $\leq$4° in visual angle. Visual stimuli were presented individually for 1 s with an interstimulus interval of 1 s at the center of the receptive field against a homogeneous gray background. The stimuli were presented once in a pseudorandom order within a stimulus presentation block. Ten blocks were presented for each recording site.

Lv as a measure for local variation of interspike intervals

To analyze firing patterns in a standardized manner, the recorded spike sequences were segmented into fragments consisting of 100 consecutive ISIs. For each neuron, if the total number of segments was $\geq$30, we took the first 30 sequences for analysis. Neurons whose spike rates were too low to provide 30 sequences were omitted. The minimum spike rate among the accepted neurons was 2.2 spikes/s. The population mean of the spike rate among accepted neurons was 8.5 spikes/s (SD 8.9; $n = 288$). Thus in the first of our analyses, we analyzed continuous spike sequences of 100 ISIs without regard to stimulus events; the sequences included spikes during stimulus presentations and spikes during interstimulus intervals.

For each set of 100 consecutive interspike intervals, the coefficient of variation *Cv* and the measure of local variation *Lv* were computed. *Cv* is defined as

$$Cv = \frac{\Delta T}{\bar{T}} \tag{1}$$

where ΔT and $\bar{T}$ are, respectively, the SD and the mean of the 100 ISIs. For a series of intervals that are independently exponentially distributed, $Cv = 1$ in the limit of a large number of intervals. For a regular spike sequence in which T_i is constant, $Cv = 0$.

Lv is defined as

$$Lv = \frac{1}{n-1}\sum_{i=1}^{n-1}\frac{3(T_i - T_{i+1})^2}{(T_i + T_{i+1})^2} \tag{2}$$

where T_i is the ith ISI, and n is the number of ISIs (in this study, $n = 100$) (Shinomoto et al. 2003). The summand is proportional to the square of $Cv_2 \equiv 2|T_1 - T_2|/(T_1 + T_2)$, which has been introduced for the purpose of comparing the temporal ISI randomness of neurons (Holt et al. 1996). The factor 3 is included here so that for a series of intervals that are independently exponentially distributed, $Lv = 1$. For a regular spike sequence in which T_i is constant, $Lv = 0$. In this way, both *Cv* and *Lv* adopt a value of 1 for a sufficiently long Poisson (random) series of events, and a value of 0 for a sequence of perfectly regular intervals. *Cv* represents the global variability of an entire ISI sequence and is sensitive to firing rate fluctuations. *Lv* represents the local stepwise variability of ISIs and depends less on the firing rate modulation (Shinomoto et al. 2005).

RESULTS

A total of 288 neurons were analyzed, with 63, 124, 44, and 57 neurons analyzed for monkeys 1–4, respectively. From the

values of *Cv* and *Lv* computed for 30 sequences of 100 ISIs, the medians were taken as the representative *Cv* and *Lv* values for each neuron. For the present data, the median values are almost identical to the mean values for individual neurons, and the following results change little if the median values are replaced with the mean values. The distributions of the median *Cv* and *Lv* values for the 288 neurons are plotted in Fig. 2. The distribution of *Lv* for the summed data from all monkeys exhibits 2 distinct peaks, whereas the *Cv* shows a unimodal distribution for the summed data (*far right panels*). The bimodality of the *Lv* distribution was observed individually for monkeys 1, 3, and 4. The *Lv* distribution for monkey 2 was not distinctly bimodal, but exhibited a tendency toward bimodality. The component distributions for the neurons in layers II–III, IV, and V–VI are shown as colored broken lines. The distribution of *Cv* was statistically distinguishable among different layers (Kruskall–Wallis, $P < 10^{-3}$) but substantially overlapped with each other. The distribution of *Lv* values also differed between layers (Kruskall–Wallis, $P < 10^{-7}$) and was clearly distinguishable between layer II–III neurons and layer V–VI neurons. The spike sequences recorded from layers II–III and layers V–VI mainly clustered in regions of larger and smaller *Lv* values, respectively. Layer IV neurons did not show this bias in *Lv* distribution. These results suggest that neurons in layers II–III and neurons in layers V–VI exhibit different firing patterns.

Cell classification according to Lv

We fitted 2-component Gaussian mixture distribution functions to the set of *Lv* values obtained from electrophysiological recordings (Fig. 3*A*, APPENDIX). For monkeys 1–4, the centers of the 2 components resulting from this fit were {1.60, 1.07}, {1.50, 0.93}, {1.46, 0.92}, and {1.66, 0.96}, respectively. The 2 Gaussian components fitted to the summed data for all monkeys were centered at 1.56 and 0.98, with weights of 0.55 and 0.45, and SDs of 0.22 and 0.21. For the purpose of categorizing neurons, we used this 2-component Gaussian fit and determined a cutoff value of *Lv* that defines the classification boundary. Neurons with *Lv* values above and below this boundary are classified into separate groups. We assume that the classification boundary θ minimizes the total areas of the 2 Gaussian tails that are on the "wrong" sides, relative to the cutoff θ. This is mathematically identical to seeking the value of *Lv* at which the 2 component distributions meet. In the summed data for all monkeys, the classification boundary θ was 1.25, yielding a theoretical misclassification rate of 8.7%. The optimal cutoff determined through this procedure was nearly identical to the value of the midway point between the centers of the 2 components, $(1.56 + 0.98)/2 = 1.27$. The following results were obtained by classifying all data from all the monkeys with the cutoff value $\theta = 1.25$. The results did not change when we adopted the cutoff value of 1.27.

The firing patterns characterized by larger values of the local variation $Lv > 1.25$, and typically localized near $Lv \approx 1.6$ are termed "clumpy-bursty" because the spikes clump together in a bursty fashion. The firing patterns characterized by smaller values of the local variation $Lv < 1.25$, particularly localized near $Lv \approx 1.0$, are termed "likely random" because a Poisson (random) spike sequence is characterized by $Lv \approx 1$. The rastergrams in Fig. 3*B* show sample spike sequences of 20 "likely random" firing neurons ($0.6 < Lv < 1.1$) and 20 "clumpy-bursty" firing neurons ($1.3 < Lv < 1.9$). The diagrams cover 2 cycles of stimulus and interstimulus periods randomly chosen from recordings from these neurons. Clumpiness of spikes captured by *Lv* is unlikely to reflect stimulus-evoked bursty responses, but reflects spikes occurring in clumps irrespective of stimulus events (Fig. 3*B*, *right*). This issue will be treated later in more detail.

Note here that $Lv = 1$ or $Cv = 1$ does not necessarily guarantee the intervals to be independently exponentially distributed. For example, even a deterministic spike sequence in which short intervals alternate with long intervals with no variation in the sequencing or the 2 interval lengths can yield $Lv = 1$ or $Cv = 1$. However, the spike sequences in TE neurons with $Lv \approx 1$ appeared to be random (Fig. 3*B*, *left*). In addition, the spike sequences with $Lv \approx 1$ tended to exhibit *Cv* significantly >1 (Fig. 2*A*). This observation is consistent with the previous analytical and simulation results that *Cv* is ≥1 for any time-dependent Poisson (random) processes with rate fluctuation over time (Shinomoto and Tsubo 2001; Shinomoto et al.

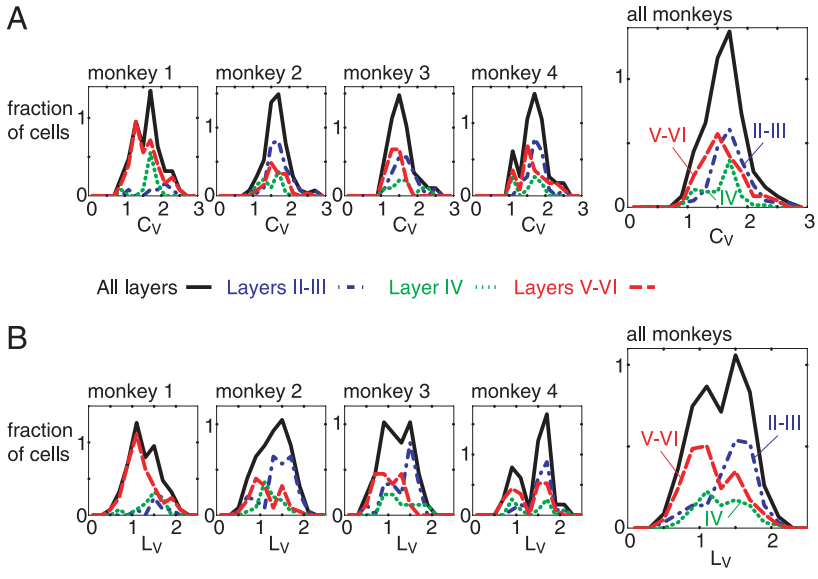

FIG. 2. Distributions of *Cv* (*A*) and *Lv* (*B*) values for area TE of monkeys 1–4 and the summed data for all monkeys. "Fraction of cells" is the number of cells counted in each bin of width $\Delta = 0.2$, divided by the total number of cells and Δ (=0.2). Data from all layers, layers II–III, layer IV, and layers V–VI are depicted as black solid, blue dot-dashed, green dotted, and red dashed lines, respectively.

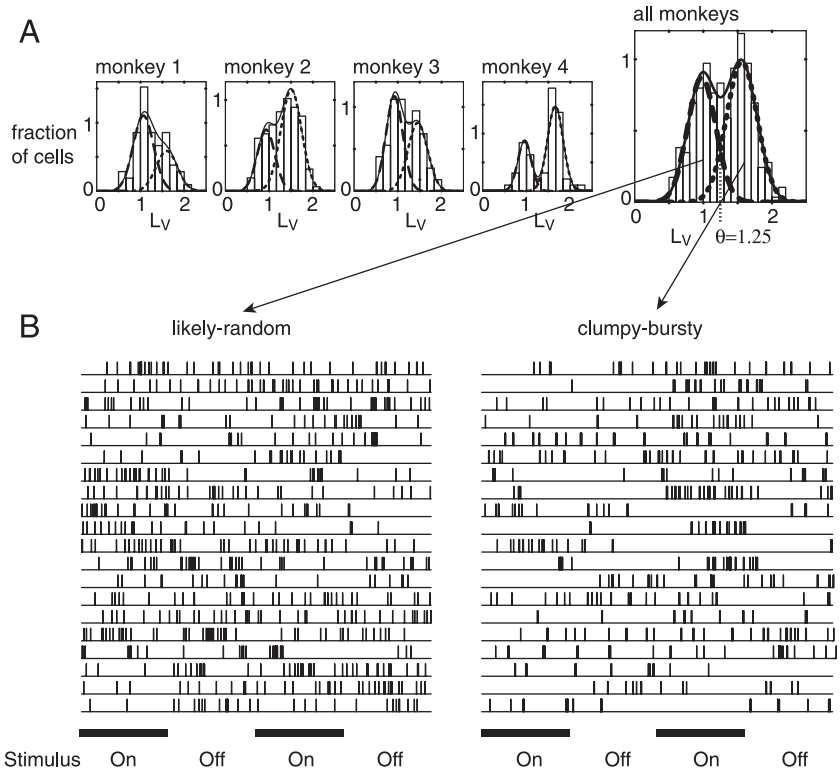

FIG. 3. *A*: 2-component Gaussian distributions fitted to the set of *Lv* values for monkeys 1–4 and the summed data for all the monkeys. Original data were plotted as histograms, fitted 2 Gaussian distributions were depicted as dotted lines, and the sum of the 2 Gaussian distributions was depicted as a solid line. *B*: sample raster diagrams of 20 "likely random" firing neurons of $0.6 < Lv < 1.1$ and 20 "clumpy-bursty" firing neurons of $1.3 < Lv < 1.9$. Each vertical bar indicates time of occurrence of a spike. Each raster contains 20–50 spikes. Clumpy-bursty rasters appear to have considerably fewer than the real number of spikes because the spikes clump together in time.

2005). The "likely random" firing patterns are also observed in the medial motor area and the prefrontal cortex, whose values of local variation are $Lv \approx 0.8$ (Shinomoto et al. 2003). "Clumpy-bursty" patterns characterized by large $Lv \approx 1.6$ are rare in the medial motor areas or the lateral prefrontal cortex. In the medial motor areas, there are neurons that exhibit spike sequences of smaller values of local variation (typically $Lv \approx 0.4$). Such spike sequences can be distinguished from the "likely random", and were termed "quasi-regular." In striking contrast, few TE neurons showed the quasi-regular patterns characterized by such small values of *Lv*.

The experiments examining neurons in the medial motor and lateral prefrontal cortices were done on awake, behaving monkeys. We then addressed whether the difference in the anesthetized versus awake monkeys caused the difference in *Lv* between the present and previous results. We analyzed the spike sequences recorded in area TE of awake monkeys, which gazed at a fixed point on a display (Kumano et al. 2001). TE neurons were tested for binocular disparity embedded in circular patches of random-dot stereograms presented parafovealy at a 2° visual angle. The *Lv* calculations for the neurons from this experiment showed a bimodal distribution with peaks at 1.0 and 1.6, which is consistent with the results obtained from anesthetized monkeys in the present study.

Lv as a measure for neuron-specific firing characteristics

A measure can be considered specific to an individual neuron if the variation in its value over time for any given neuron is small in comparison with the variation in its value among different neurons. To determine the amount by which *Lv*, *Cv*, and the mean of interspike intervals $\bar{T}$ vary in time, we used a scatter graph to plot pairs of values for each measurement obtained from 2 sequences of the 100 ISIs recorded from a single neuron (Fig. 4, *A–C*). We picked the 1st and 15th sequences from the 30 sequences of the 100 ISIs measured for each of the 288 neurons. The results are not significantly altered by choosing a different pair of sequences. For the present experimental data, the recorded spike rate was typically 8.5 spikes/s, meaning that the time period needed to obtain one sequence of the 100 ISIs is about $100/8.5 \approx 12$ s, and the time interval between the 1st and 15th sequence is 180 s. Two values of *Lv* determined from different time periods exhibited a strong correlation ($r = 0.85$, $n = 288$). The observed variation of *Lv* among neurons was larger than the variation within neurons ($F = 185.615$, $P < 0.001$; ANOVA). In contrast, *Cv* as well as $\bar{T}$ exhibited a weaker correlation ($r = 0.52$ and 0.48, $n = 288$).

We also examined the skewness coefficient (*SK*), a measure for the asymmetry of the ISI distribution (Shinomoto et al. 1999). *SK* showed a much weaker correlation ($r = 0.18$, $n = 288$, data not shown) between 2 values determined at different time periods. In addition, we examined the correlation coefficient of consecutive intervals (*COR*) (Sakai et al. 1999). For any renewal process, *COR* is normally distributed with the zero

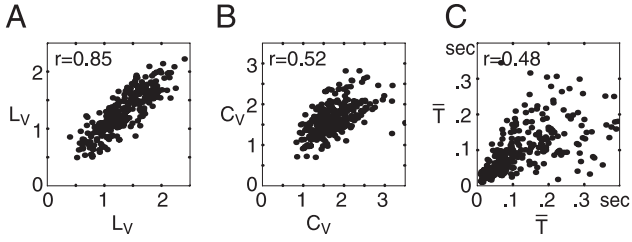

FIG. 4. Scattergrams of the local variation *Lv* (*A*), the coefficient of variation *Cv* (*B*), and the mean interspike interval $\bar{T}$ (*C*), for 2 sequences of 100 ISIs from different time periods, each sampled from the same neuron. Each dot denotes data from a single neuron. $n = 288$.

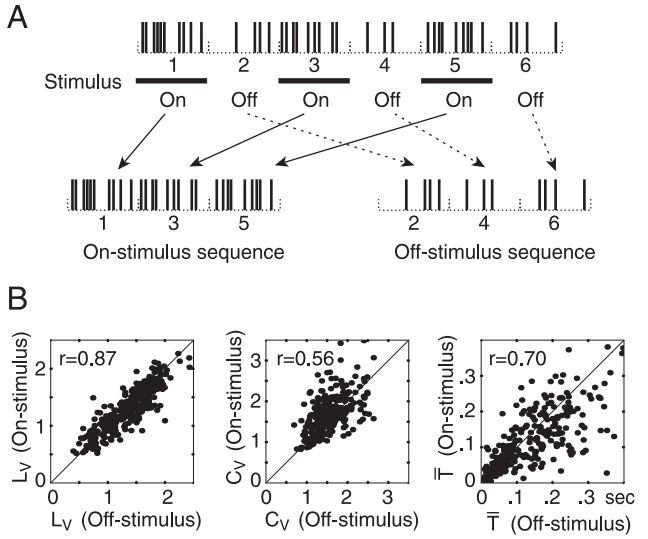

FIG. 5. *A*: schema for concatenating spike sequences of stimulus periods and interstimulus periods, respectively, to construct stimulus-present and stimulus-absent spike sequences. *B*: scattergrams of the local variation *Lv* (*left*), the coefficient of variation *Cv* (*center*), and the mean interspike interval $\bar{T}$ (*right*), for 2 sequences of 100 ISIs from the stimulus-present and stimulus-absent spike sequences, each derived from the same neuron.

mean, and the variance of $1/n$ in the case of a large number of intervals (Cox and Lewis 1966). The mean value of the *COR* for our data were 0.08 ($n = 99$), indicating that the consecutive intervals were not significantly correlated ($P > 0.05$). The pairs of *COR* values obtained from 2 sequences of 100 ISIs were also very weakly correlated ($r = 0.12$, $n = 288$, data not shown). These results suggest that *Lv* is better suited for characterizing firing characteristics specific to individual neurons than the other measures.

Effects of stimulus events on Lv

The results in Fig. 4 suggest that *Lv* can be an indicator of an inherent spiking property of neurons. This analysis, however, was performed on spike sequences spanning both stimulus-present and stimulus-absent periods without any consideration of effects of visually driven responses on *Lv*. We next addressed to what extent *Lv* depends on stimulus events and how it relates to various aspects of visual responses.

We first asked whether *Lv* in individual neurons differs between stimulus-present periods and stimulus-absent periods. We computed *Lv* separately for stimulus periods and interstimulus intervals in each neuron. Because the number of spikes in a single 1-s stimulus period or 1-s interstimulus interval was too small to obtain a reliable estimate of these coefficients, we concatenated spike sequences of stimulus periods and interstimulus intervals, respectively, to construct the stimulus-present and stimulus-absent spike sequences (Fig. 5*A*).

Figure 5*B* shows *Lv*, *Cv*, and the mean interspike interval computed from the first 100 ISI sequences of stimulus-present and stimulus-absent periods for the 288 neurons. The 2 values of *Lv* exhibited a strong correlation ($r = 0.87$) and distributed tightly around the diagonal line, indicating that *Lv* was preserved between stimulus-present and stimulus-absent periods. *Cv* exhibited a weaker correlation ($r = 0.56$). In contrast, $\bar{T}$ values of the off-stimulus spike sequences were on average about 1.2 times larger than those of the on-stimulus spike sequences, stemming from the visually evoked spike rate change.

On average, only 15% of the 64 stimuli evoked statistically significant responses, and the other stimuli were ineffective in our TE neurons (Tamura et al. 2004), raising the possibility that most of the "stimulus-present" periods may really be "no-stimulus" periods for the neurons. We then computed *Lv* separately for effective-stimulus periods ($P < 0.05$, Wilcoxon signed-rank test) and for interstimulus intervals. This analysis was performed for 194 of the 288 neurons that provided a sufficient number of spikes (30 sequences of 10 ISIs) for calculation of *Lv* for effective-stimulus periods and for interstimulus intervals. Figure 6 plots *Lv* and mean ISI ($\bar{T}$) for visual responses during effective stimulus periods and interstimulus intervals of each neuron. *Lv* measured during the 2 periods showed a strong correlation ($r = 0.76$ for $n = 154$ layer II–III and layer V–VI neurons, $r = 0.89$ for $n = 154 + 40$ layer IV neurons; both $P < 0.001$); whether the measurement of *Lv* is from visual responses or ongoing discharges, individual neurons show a consistent *Lv*. *Lv* during effective-stimulus periods was slightly smaller than that during ineffective-stimulus interstimulus intervals in each neuron. Across the population of neurons, neurons with a stronger firing rate (i.e., a smaller $\bar{T}$) showed a smaller *Lv* ($r = -0.61$).

The correlation between *Lv* and the firing rate raises the possibility that the observed laminar difference of *Lv* (Fig. 2*B*) might be derived from a laminar difference of the firing rate. Indeed, the firing rate differed among layers (7.0 + 6.9 spikes/s for layer II–III neurons, 8.9 + 7.2 spikes/s for layer IV neurons, 9.6 + 7.6 spikes/s for layer V–VI neurons; $P < 0.001$, Kruskal–Wallis test). We applied ANCOVA to these data to examine whether *Lv* differs after the variation attributed to the

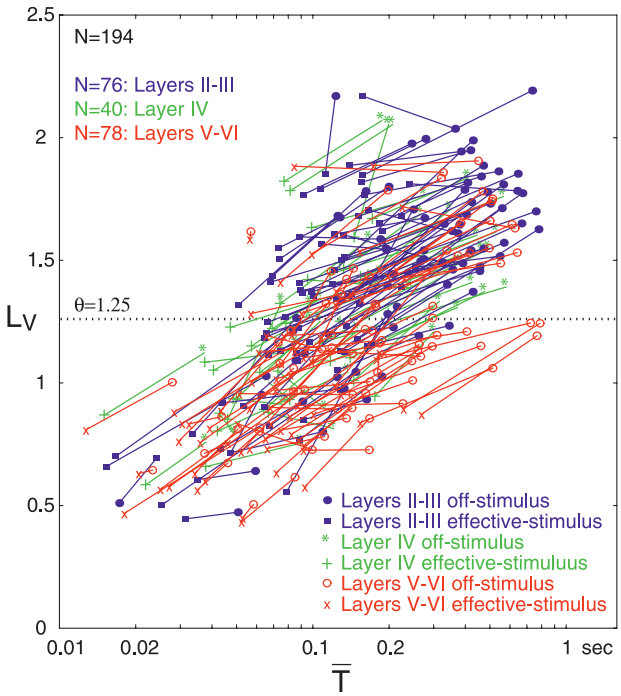

FIG. 6. Scatter plot of *Lv* and $\bar{T}$ for effective-stimulus periods and interstimulus periods. Each line shows data from each of the 194 neurons analyzed. Blue lines indicate data from layer II–III neurons, green lines those from layer IV neurons, and red lines those from layer V–VI neurons.

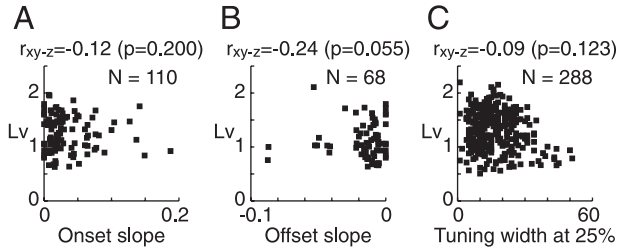

FIG. 7. *A*: relationship between *Lv* and the slope of response onset. Three points with a large slope are not included in the graph. *B*: relationship between *Lv* and the slope of response offset. See text for definition of the slope of response onset and offset. *C*: relationship between *Lv* and the number of stimuli that evoked responses >25% of the maximal response. Correlation coefficient or partial correlation coefficient is provided as r or r_{xy-z} with corresponding P values.

covariate (i.e., firing rate) is compensated. We found that there was a significant difference in *Lv* among layers ($P < 0.001$, ANCOVA).

In example neurons shown in Fig. 3*B*, *Lv* is unlikely related to spike rate transitions at stimulus onsets and offsets. We now addressed the relationship between *Lv* and sharpness of spike rate transients at stimulus onsets and offsets for a population of neurons. In this analysis, sharpness of the response onset and offset is defined as the slope of linear regression line fitted to portions of peristimulus time histograms spanning 80 to 200 ms after the stimulus onset or offset, respectively. Only responses with significant regression ($P < 0.05$) were subjected to further analysis. Because the slope was correlated with the firing rate ($r = 0.224$, $P = 0.019$ for onset slope; $r = -0.323$, $P = 0.007$ for offset slope), and as we have described above, *Lv* was correlated with the firing rate, we calculated partial correlation coefficient between *Lv* and the slope by removing the effects of the firing rate (r_{xy-z}). Analysis of partial correlation coefficients allowed us to examine the net correlation between *Lv* and the slopes by removing the effect of the firing rate. This analysis indicates that *Lv* was not correlated with the slopes of the response onset or offset (Fig. 7, *A* and *B*; $r_{xy-z} = 0.12$, $P = 0.200$, $n = 110$ for onset slope; $r_{xy-z} = 0.24$, $P = 0.055$, $n = 68$ for offset slope).

Finally we examined relationship between *Lv* and stimulus selectivity. As a measure of stimulus selectivity we used the number of stimuli that evoked responses >25% of the maximal response (Tamura et al. 2004). Because the measure of stimulus selectivity was also correlated with the firing rate ($r = 0.19$, $P = 0.001$, $n = 288$), we calculated partial correlation coefficient between *Lv* and the measure of stimulus selectivity by compensating the effects of firing rate. *Lv* did not correlate with the measure of stimulus selectivity (Fig. 7*C*; $r_{xy-z} = -0.09$, $P = 0.123$).

The results indicate that neurons retain the firing characteristics captured by *Lv* to a large extent regardless of stimulus events and associated transient changes in firing rates. However, *Lv* did negatively correlate with the firing rate both within a neuron and across a population of neurons. This may be partly because ISIs inevitably take a smaller range of variation with an increase in the overall firing rate.

Lv and burst firing

We next analyzed the frequency of burst firings. We defined 2 consecutive short intervals <5 ms each as a "unit burst," and calculated the rate of bursts R_b as the number of such "unit bursts" divided by the total number of 2 consecutive intervals $n - 1$, for a single sequence of 100 ISIs. A Poisson process with a mean ISI of 120 ms (i.e., 8.5 spikes/s) is expected to yield a very low rate of bursts

$$R_b = \left(\int_0^5 \mathrm{d}t/120 \exp[-t/120] \right)^2 \approx 0.002$$

However, our recorded spike sequences exhibited R_b values significantly larger than this (Fig. 8*A*; range 0–0.67, mean 0.034, median 0.010, $n = 8{,}640$ sequences = 30 sequences × 288 neurons). A pair of R_b values determined for 2 sequences of the 100 ISIs obtained at different time periods from a single neuron were correlated with each other ($r = 0.67$, $P < 0.0001$, $n = 288$; Fig. 8*B*), indicating that bursting is also a fairly specific character of individual neurons. *Lv* was also correlated with the R_b ($r = 0.25$, $P < 0.0001$; Fig. 8*C*); neurons with larger *Lv* more often show the burst firing defined above than neurons with smaller *Lv*.

Spike width of "clumpy-bursty" and "likely random" firing neurons

We next examined how GABAergic inhibitory interneurons, which constitute 20–25% of the total population of cortical neurons (Gabbott and Somogyi 1986; Hendry et al. 1987), are distributed over "clumpy-bursty" and "likely random" firing neurons. It is known that neurons producing short-duration action potentials are likely to be interneurons, although the opposite is not necessarily true (Kawaguchi 1995; Tamura et al. 2004). Figure 9*A* depicts sample action potentials recorded from area TE. We define the spike width as the duration of time from the initial negative trough to the subsequent positive peak. Figure 9*B* shows the joint distribution of spike widths and the values of *Lv* for the 288 neurons. A small hump in the spike width distribution with a short-duration of about 0.3 ms may correspond to fast-spiking interneurons. Most neurons with such thin action potentials exhibited "likely random" firing patterns. However, the opposite is not necessarily true; "likely random" firing neurons did not necessarily produce thin action potentials. Figure 9*C* depicts the spike width distribution for different cortical layers. All layers contain neurons of thin and thick action potentials, but the layers V–VI contain relatively larger fraction of neurons of thin action potentials than other layers.

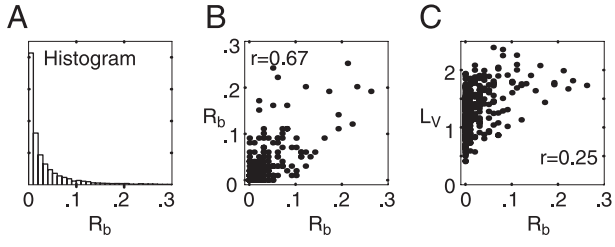

FIG. 8. *A*: histogram of the rates of bursts R_b for all recorded sequences of 100 ISIs. Although the data ranged from 0 to 0.67, the number of 100 ISI sequences of R_b >0.3 was very small (114 out of 8526, 1.3%) and is not pictured here. *B*: scattergram of R_b for 2 sequences of 100 ISIs in different time periods, each sampled from the same neuron. *C*: scattergram of R_b–*Lv* for the same sequences of 100 ISIs individually sampled from the 288 neurons.

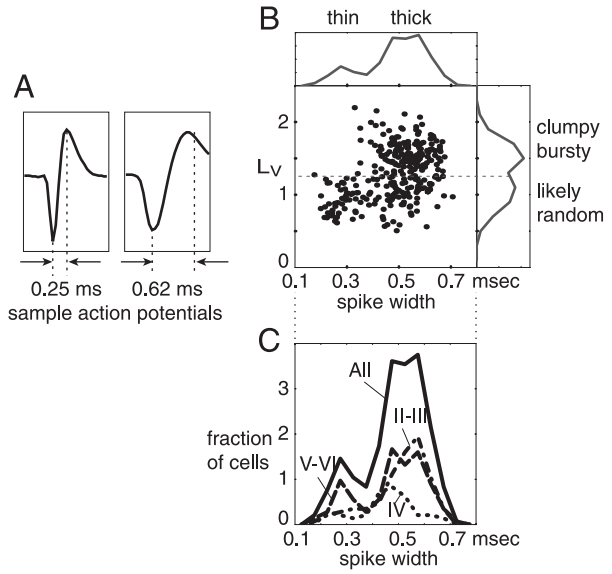

FIG. 9. *A*: 2 examples of spike shapes with short and long widths. *B*: distribution of the spike widths and the *Lv* values of the 288 neurons. *C*: distributions of the spike widths from all layers, layers II–III, layer IV, and layers V–VI, depicted as solid, dot-dashed, dotted, and dashed lines, respectively.

DISCUSSION

We characterized the firing patterns of TE neurons by calculating *Lv*, the local variation of interspike intervals. *Lv* did not vary significantly in time for any given neuron in comparison with its variation between different neurons. The distribution of *Lv* was bimodal, allowing us to classify TE neurons into 2 groups. One group of neurons had a mean *Lv* of 0.98 and fired in a random fashion. The other group of neurons had a mean *Lv* of 1.56 and their spikes clustered in clumps. We found that layer II–III neurons had larger *Lv* values and were classified as the "clumpy-bursty" firing type, whereas layer V–VI neurons had a smaller *Lv* and were classified as the "likely random" firing type (Table 1). This laminar difference persisted after compensating for the effect of the firing rate on *Lv*.

Two types of TE neurons with different Lv values

Comparison of *Lv* with the mean and the conventional coefficient of variation (*Cv*) of ISIs indicates that *Lv* represents the spiking characteristics specific to individual neurons more reliably than the other measures we tested. When we determined *Lv* values for 2 sequences of 100 ISIs, each selected from recordings of individual TE neurons, they were strongly correlated ($r = 0.85$). Similar correlations of *Lv* values have been seen in the medial frontal cortex, or medial motor areas ($r = 0.78–0.85$), although lateral frontal cortex neurons show a weaker correlation ($r = 0.59$) (Shinomoto et al. 2003). More important, the bimodal distribution of *Lv* with peaks at $Lv = 1.0$ and 1.6 was preserved under drastically different experimental conditions, one in which responses of TE neurons were tested with a variety of shapes and photographs in anesthetized monkeys (Tamura et al. 2004) and the other in which they were tested using a range of disparities embedded in dynamic random dot stereograms in awake, fixating monkeys (Kumano et al. 2001). These results suggest that *Lv* reflects an aspect of the in vivo firing pattern of these neurons that is largely unaffected by the type of visual stimuli presented and the experimental conditions.

The neuron-specific firing patterns may be intrinsically determined by the membrane properties of individual cell types. Cortical neurons produce specific firing patterns in response to intracellularly applied depolarizing current pulses, indicating that this aspect of the firing characteristic is intrinsic to cells (e.g., Kawaguchi 1995; McCormick et al. 1985; for reviews, see Amitai and Connors 1995; Connors and Gutnick 1990). However, it is also possible that the input-feeding circuit differs among TE neurons, and that this contributes to the differences in firing patterns captured by *Lv* measurements. The microorganization of afferent input pathways differs between cells within a cortical area or even cells residing in the same layer of the same cortex (Callaway 2002; Thomson and Deuchars 1997; Thomson and Morris 2002).

Other classification schemes of cortical firing patterns

Previous work has classified cortical neurons according to firing type under both in vitro and in vivo conditions (e.g., Gray and McCormick 1996; Kawaguchi 1995; McCormick et al. 1985; Mountcastle et al. 1969; Nowak et al. 2003; Simons 1978). By applying cluster analysis to intracellular responses to pulses of electric current, Nowak et al. (2003) classified neurons in the cat primary visual cortex into regular spiking, intrinsic bursting, chattering, and fast spiking types. The first 3 represent spiny pyramidal and stellate cells and are presumed to be excitatory neurons, whereas the last type represents aspinous or poorly spinous neurons and is presumed to be inhibitory. In addition, Kawaguchi (1995) classified nonpyramidal neurons in layer II/III of the rat frontal cortex into fast-spiking cells, late-spiking cells, low-threshold spike cells, and regular-spiking nonpyramidal cells. These physiological types correspond to specific classes of inhibitory interneurons with distinct morphological and neurochemical characteristics. It is not readily obvious if any of these cell types correspond to any of the cell types defined by *Lv* for extracellularly recorded spike trains. At present, we do not see any simple correlation between the 2 classification schemes. For example, chattering cells share some features with "clumpy-bursty" firing neurons, in that they fire in bursty fashion and are distributed predominantly in layer II/III (Nowak et al. 2003). Chattering cells, however, have shorter-duration action potentials, whereas "clumpy-bursty" firing neurons have broader action potentials (Fig. 9).

Layer distribution of "clumpy-bursty" and "likely random" firing neurons

Layer localization of neurons recorded in physiological experiments provides an important clue to understanding how information is processed in the cortex. However, except for the

TABLE 1. *Two types of in vivo firing patterns in area TE*

Firing Type	*Lv*	Layer Localization	Spike Width
Clumpy-bursty	1.56	2/3 dominant	Thick
Likely random	0.98	5/6 dominant	Thin and thick

"*Lv*" is the estimated peak position of the fitted Gaussian function of *Lv* distribution.

primary visual cortex where the laminar distribution of receptive field properties is well documented (Snodderly and Gur 1995), it is usually difficult to determine during such experiments from which layer the neuronal recording is being made. The differential, although not perfectly distinct, distribution of "clumpy-bursty" and "likely random" firing neurons in layers II–III versus layers V–VI can help in identification of the recorded layer. In particular, simultaneous recordings from multiple neurons at a site would make this laminar estimation more reliable. Making a linkage between spiking patterns based on *Lv* and anatomically defined neuronal type, by using juxtacellular labeling techniques for instance, will be an important research direction in future studies.

Heterogeneity of cortical areas

The distribution patterns of *Lv* for neurons in area TE and the medial motor areas are both bimodal, but the peak positions differ markedly between them (Fig. 10). We showed that "clumpy-bursty" and "likely random" firing neurons in area TE are characterized by $Lv = 1.56$ and $Lv = 0.98$, respectively, whereas previous work showed that 2 types of neurons in the medial motor areas are characterized by $Lv = 0.81$ (likely random) and $Lv = 0.38$ (quasi-regular) (Shinomoto et al. 2003). The *Lv* distribution of the lateral prefrontal cortex is not distinctly bimodal, but it is also best fit by 2 Gaussian distributions of the mean $Lv = 0.83$ and $Lv = 0.58$ (Shinomoto et al. 2003). All 3 areas thus contain a neuronal population with *Lv* close to 1, suggesting that the random-firing type is common across cortical areas. In contrast, the "clumpy-bursty" firing neurons observed in area TE are rarely observed in the medial motor and lateral prefrontal cortices. Conversely, the "quasi-regular" firing patterns observed in the medial motor areas are rarely observed in area TE.

Different experiments used different types of electrodes and may have a specific bias in sampling of the neurons. The recording of the anesthetized monkeys was performed using electrodes with 7 recording probes (Heptode, Thomas; impedance 1–2 MΩ at 1 kHz), whereas the recording of the awake monkeys was carried out by using conventional metal microelectrodes (FHC, Bowdoinham, ME; impedance 1 MΩ at 1 kHz). The latter is similar to those used for experiments in the medial motor area (custom-made, glass-insulated Elgiloy-alloy electrodes; impedance 1.5–3 MΩ at 1 kHz; see Shinomoto et al. 2003). Data recorded from the same cortical area with different types of electrodes exhibited similar *Lv* distributions, whereas the data recorded from different cortical areas with similar types of electrodes exhibited distinctly different *Lv* distributions. The difference of *Lv* distributions between the medial motor and lateral frontal cortices and area TE is thus unlikely to be caused by a sampling bias, but represents a genuine difference between them.

According to morphological criteria, the same basic types of neurons are found in all cortical areas. In addition, the proportion of γ-aminobutyric acid (GABA) neurons to pyramidal neurons is preserved across different areas of the cerebral cortex (Hendry et al. 1987), and no differences in electrophysiological membrane properties have been detected between sensorimotor and anterior cingulate cortices (McCormick et al. 1985). Furthermore, different cortical areas share many of the basic statistical features of firing (Shadlen and Newsome 1998). However, in spite of these similarities, recent studies have begun to elucidate differences in the structural and physiological organization across different areas of the cortex. Morphological characteristics of pyramidal neurons (such as the size and complexity of dendritic arbors; the number of dendritic spines; and the size, shape, and distribution of clusters of horizontal axon arborization) differ between cortical areas, suggesting that the strategy of input sampling and dissemination differ among them (Amir et al. 1993; Benavides-Piccione et al. 2002; Lund et al. 1993; Tanigawa et al. 2005; for reviews, see Elston 2002; Fujita 2002). It remains to be determined whether some of these differences are related to the differences in *Lv* between the temporal cortex and the medial motor and lateral prefrontal cortices. What roles these different firing patterns might play in different kinds of processing in different cortical areas should also be addressed in future studies. If we could obtain a map of the entire brain with respect to firing characteristics, we would be able to have a

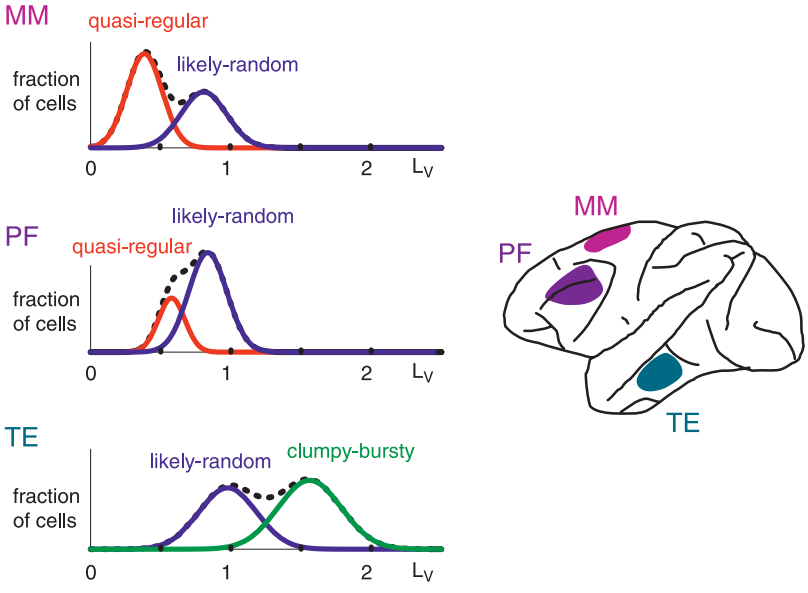

FIG. 10. Various types of spike sequences categorized according to *Lv* values. Centers of the fitted 2-component Gaussian distributions of *Lv* for the medial motor areas MM, the prefrontal cortex PF, and area TE of the inferior temporal cortex are located at {0.8 (likely random), 0.4 (quasi-regular)}, {0.8 (likely random), 0.6 (quasi-regular)}, and {1.6 (clumpy-bursty), 1.0 (likely random)}, respectively. Data for MM and PF are from Shinomoto et al. (2003).

better insight into the relationship between firing properties and the functional roles of neurons.

APPENDIX

Gaussian mixture distribution

Because the distribution of *Lv* values was bimodal, we fitted a 2-component Gaussian mixture distribution function to this set of values. The methods and the criteria used for 2-component Gaussian distributions were the same as those used by Shinomoto et al. (2003).

The 2-component Gaussian mixture distribution is defined as

$$p(x) = w_1 N(x|\mu_1, \sigma_1^2) + w_2 N(x|\mu_2, \sigma_2^2) \quad (A1)$$

where $N(x|\mu, \sigma^2)$ is the Gaussian (normal) distribution of mean μ and variance σ^2, and $w_1 > 0$ and $w_2 = 1 - w_1 > 0$ are the weights of the 1st and 2nd component distributions. This distribution is fitted to a data set $\{x_1, x_2, \ldots, x_p\}$ by locally maximizing the log-likelihood

$$l = \sum_{j=1}^{p} \ln p\,(x_j) \quad (A2)$$

with respect to 5 parameters, $\theta = \{\mu_1, \sigma_1^2, \mu_2, \sigma_2^2, w_1\}$. Fitting of the Gaussian mixture distribution can also be carried out by the expectation maximization (EM) algorithm (Dempster et al. 1977). The distribution functions fitted to the individual data sets are shown in Fig. 3*A*.

ACKNOWLEDGMENTS

Thanks to H. Kaneko, M. Murayama, and K. Miyata for technical assistance in the neurophysiological experiments and to S. Tate for help in data analysis. We also thank J. Tanji and K. Shima for kind help with the recorded area map in Fig. 7.

GRANTS

This work was supported in part by grants from the Japanese Ministry of Education, Culture, Sports, Science and Technology to S. Shinomoto, I. Fujita, and H. Tamura; a Core Research for the Evolutional Science and Technology Program grant from the Japan Science and Technology Corporation to I. Fujita; and a Grant-in-Aid for the 21st Century COE, "Center for Diversity and Universality in Physics" to S. Shinomoto.

REFERENCES

Amir Y, Harel M, and Malach R. Cortical hierarchy reflected in the organization of intrinsic connections in macaque monkey visual cortex. *J Comp Neurol* 334: 19–46, 1993.

Amitai Y and Connors BW. Intrinsic physiology and morphology of single neurons in neocortex. In: *Cerebral Cortex*, edited by Jones EG and Diamond IT. New York: Plenum, 1995, vol. 11.

Benavides-Piccione R, Ballesteros-Yánez I, DeFelipe J, and Yuste R. Cortical area and species differences in dendritic spine morphology. *J Neurocytol* 31: 337–343, 2002.

Buzsáki G, Leung LS, and Vanderwolf CH. Cellular bases of hippocampal EEG in the behaving rat. *Brain Res Rev* 6: 139–171, 1983.

Callaway EM. Cell type specificity of local cortical connection. *J Neurocytol* 31: 231–237, 2002.

Conners BW and Gutnick MJ. Intrinsic firing patterns of diverse neocortical neurons. *Trends Neurosci* 13: 99–104, 1990.

Constantinidis C, Williams GV, and Goldman-Rakic PS. A role for inhibition in shaping the temporal flow of information in prefrontal cortex. *Nat Neurosci* 5: 175–180, 2002.

Cox DR and Lewis PAW. *The Statistical Analysis of Series of Events.* London: Methuen, 1966.

Csicsvari J, Hirase H, Czurkó A, and Buzsáki G. Reliability and state dependence of pyramidal cell–interneuron synapses in the hippocampus: and ensemble approach in the behaving rat. *Neuron* 21: 179–189, 1998.

Dempster A, Laird N, and Rubin D. Maximum likelihood from incomplete data via the EM algorithm. *J R Stat Soc Ser B* 39: 1–38, 1977.

Elston GN. Cortical heterogeneity: implication for visual processing and polysensory integration. *J Neurocytol* 31: 317–335, 2002.

Fujita I. The inferior temporal cortex: architecture, computation, and representation. *J Neurocytol* 31: 373–385, 2002.

Fujita I and Fujita T. Intrinsic connections in the macaque inferior temporal cortex. *J Comp Neurol* 368: 467–486, 1996.

Gabbot PL and Somogyi P. Quantitative distribution of GABA-immunoreactive neurons in the visual cortex (area 17) of the cat. *Exp Brain Res* 61: 323–331, 1986.

Gray CM and McCormick DA. Chattering cells: superficial pyramidal neurons contributing to the generation of synchronous oscillations in the visual cortex. *Science* 274: 109–113, 1996.

Hendry SHC, Schwark HD, Jones EG, and Yan J. Numbers and proportions of GABA-immunoreactive neurons in different areas of monkey cerebral cortex. *J Neurosci* 7: 1503–1529, 1987.

Holt GR, Softky WR, Koch C, and Douglas RJ. Comparison of discharge variability in vitro and in vivo in cat visual cortex neurons. *J Neurophysiol* 75: 1806–1814, 1996.

Kaneko H, Suzuki SS, Okada J, and Akamatsu M. Multineuronal spike classification based on multisite electrode recordings, whole-waveform analysis, and hierarchical clustering. *IEEE Trans Biomed Eng* 46: 280–290, 1999.

Kawaguchi Y. Physiological subgroups of nonpyramidal cells with specific morphological characteristics in layer II/III of rat frontal cortex. *J Neurosci* 15: 2638–2655, 1995.

Kumano H, Tanaka H, Uka H, and Fujita I. Disparity selectivity of monkey inferior temporal neurons as examined by dynamic random dot stereograms. *Neurosci Res Suppl* 25: s161, 2001.

Lund JS, Yoshioka T, and Levitt JB. Comparison of intrinsic connectivity in different areas of macaque monkey cerebral cortex. *Cereb Cortex* 3: 148–162, 1993.

McCormick DA, Connors BW, Lighthall JW, and Prince DA. Comparative electrophysiology of pyramidal and sparsely spiny stellate neurons of the neocortex. *J Neurophysiol* 54: 782–806, 1985.

Mountcastle VB, Talbot WH, Sakata H, and Hyvärinen J. Cortical neuronal mechanisms in flutter-vibration studied in unanesthetized monkeys. Neuronal periodicity and frequency discrimination. *J Neurophysiol* 32: 452–484, 1969.

Nowak LG, Azouz R, Sanchez-Vives MV, Gray CM, and McCormick DA. Electrophysiological classes of cat primary visual cortical neurons in vivo as revealed by quantitative analyses. *J Neurophysiol* 89: 1541–1566, 2003.

Ranck JB Jr. Studies on single neurons in dorsal hippocampal formation and septum in unrestrained rats. Part I. Behavioral correlates and firing repertoires. *Exp Neurol* 41: 461–531, 1973.

Sakai Y, Funahashi S, and Shinomoto S. Temporally correlated inputs to leaky integrate-and-fire models can reproduce spiking statistics of cortical neurons. *Neural Networks* 12: 1181–1190, 1999.

Shadlen MN and Newsome WT. The variable discharge of cortical neurons: implications for connectivity, computation, and information coding. *J Neurosci* 18: 3870–3896, 1998.

Shinomoto S, Miura K, and Koyama S. A measure of local variation of inter-spike intervals. *BioSystems* 79: 67–72, 2005.

Shinomoto S, Sakai Y, and Funahashi S. The Ornstein–Uhlenbeck process does not reproduce spiking statistics of neurons in prefrontal cortex. *Neural Comput* 11: 935–951, 1999.

Shinomoto S, Shima K, and Tanji J. Differences in spiking patterns among cortical neurons. *Neural Comput* 15: 2823–2842, 2003.

Shinomoto S and Tsubo Y. Modeling spiking behavior of neurons with time-dependent Poisson processes. *Phys Rev E* 64: 041910(1–13), 2001.

Simons DJ. Response properties of vibrissa units in rat S1 somatosensory neocortex. *J Neurophysiol* 41: 798–820, 1978.

Snodderly DM and Gur M. Organization of striate cortex of alert, trained monkeys (*Macaca fascicularis*): ongoing activity, stimulus selectivity, and widths of receptive field activating regions. *J Neurophysiol* 74: 2100–2125, 1995.

Tamura H, Kaneko H, Kawasaki K, and Fujita I. Presumed inhibitory neurons in the macaque inferior temporal cortex: visual response properties and functional interactions with adjacent neurons. *J Neurophysiol* 92: 2782–2796, 2004.

Tanigawa H, Wang QX, and Fujita I. Organization of horizontal axons in the inferior temporal cortex and primary visual cortex of the macaque monkey. *Cereb Cortex* In press.

Thomson AM and Deuchars J. Synaptic interactions in neocortical local circuits: dual intracellular recordings in vitro. *Cereb Cortex* 7: 510–522, 1997.

Thomson AM and Morris OT. Selectivity in the inter-laminar connections made by neocortical neurones. *J Neurocytol* 31: 239–246, 2002.